Geophys. J. Int. (2004) **159,** 555–564 doi: 10.1111/j.1365-246X.2004.02438.x

Magnetic quantification of urban pollution sources in atmospheric particulate matter

S. Spassov,[1,*] R. Egli,[1] F. Heller,[1] D. K. Nourgaliev[2] and J. Hannam[3]

[1] *Institut für Geophysik, ETH Zürich,* CH-8093, *Zürich, Switzerland*
[2] *Faculty of Geology, Kazan State University,* 420008, *Kazan, Russia*
[3] *Department of Geography, University of Liverpool, Liverpool* L69 7ZT, *UK*

Accepted 2004 July 21. Received 2004 June 18; in original form 2003 September 23

SUMMARY

A new method is presented for fast quantification of urban pollution sources in atmospheric particulate matter (PM). The remanent magnetization of PM samples collected in Switzerland at sites with different exposures to pollution sources is analysed. The coercivity distribution of each sample is calculated from detailed demagnetization curves of anhysteretic remanent magnetization (ARM) and is modelled using a linear combination of appropriate functions which represent the contribution of different sources of magnetic minerals to the total magnetization. Two magnetic components, C1 and C2, are identified in all samples. The low-coercivity component C1 predominates in less polluted sites, whereas the concentration of the higher-coercivity component C2 is large in urban areas. The same sites were monitored independently by Hüglin using detailed chemical analysis and a quantitative source attribution of the PM. His results are compared with the magnetic component analysis. The absolute and relative magnetic contributions of component C2 correlate very well with absolute and relative mass contributions of exhaust emissions, respectively. Traffic is the most important PM pollution source in Switzerland: it includes exhaust emissions and abrasion products released by vehicle brakes. Component C2 and traffic-related PM sources correlate well, which is encouraging for the implementation of non-destructive magnetic methods as an economic alternative to chemical analysis when mapping urban dust pollution.

Key words: component analysis, PM10, road traffic emissions, rock magnetism, Zürich.

1 INTRODUCTION

The harmful effects of anthropogenically derived particulate matter (PM) on human health have attracted the attention of environmental research in recent years. Particles <10 μm (PM10) are of special interest because they can be inhaled deeply into the lung and induce cytotoxic and inflammatory effects when iron and other heavy metals become bioavailable. Studies on residual oil fly ash (Dreher *et al.* 1997) or coal fly ash (van Maanen *et al.* 1999; Smith *et al.* 2000) have shown that the transition metals Fe, Cu, Ni or V seem to play an important role. Diabaté *et al.* (2002) suggested that the pro-inflammatory responses of the cells could be induced by metals attached to the particle surface or by a large number of fine and ultrafine particles with a large surface/volume ratio.

Since heavy metals have a high affinity towards iron oxides (Cornell & Schwertmann 1996), magnetic methods can be used for the characterization of airborne pollution (e.g. Hunt *et al.* 1984; Dekkers & Pietersen 1992; Matzka & Maher 1999; Xie *et al.* 2000; Kapička *et al.* 2001; Muxworthy *et al.* 2001; Shu *et al.* 2001; Muxworthy *et al.* 2002, 2003). Matzka (1997) and Muxworthy *et al.* (2003) found a positive correlation between the saturation magnetization of isothermal remanent magnetization (IRM) of PM10 filters and the total PM10 mass. Tree leaves in urban environments have the potential to remove the atmospheric PM because of their high surface area and suitable surface properties (Freer-Smith *et al.* 1997). The ability to map spatial distributions of anthropogenic pollution by measuring the magnetization of tree leaves has been demonstrated in different European cities (Hannam & Heller 2001; Moreno *et al.* 2003). High susceptibility is often observed in the city centre near busy roads and railway stations. In contrast, low values are found in rural regions with almost no traffic.

The urban PM consists of natural and anthropogenic components (Hüglin 2000) which are both thought to contain magnetic mineral fractions with specific magnetic properties. An earlier PM10 analysis by Muxworthy *et al.* (2001) indicated that bulk magnetic parameters such as susceptibility do not always correlate with the amount of particulate matter and may therefore be misleading for the

*Now at: Centre de Physique du Globe, Institut Royal Météorologique, Dourbes, B-5670, Belgium. E-mail: simo.spassov@oma.be

© 2004 RAS

assessment of air pollution using magnetic methods. In this work, the magnetic contribution of individual components is quantified and compared with a detailed source attribution based on chemical investigations performed by Hüglin (2000). Two major questions related to the practical application of magnetic measurements for air pollution monitoring will be addressed: (1) Can pollution sources in PM be identified quantitatively using magnetic measurements? (2) Is the concentration of potentially harmful substances, such as heavy metals, directly correlated with the magnetic properties of PM? In order to answer these questions, magnetic and chemical properties of PM10 samples collected at several sites in Switzerland and characterized by their different exposure to possible pollution sources are compared in detail.

2 SAMPLES AND MEASUREMENTS

2.1 Sampling sites

Representative sampling sites were selected with reference to previous PM10 investigations (Hüglin 2000; Hannam & Heller 2001). These sites represent important air pollution scenarios. Site CHM is located in a remote rural region in the Swiss Jura mountains near the city of Neuchâtel. It is characterized by a mean PM10 concentration (mean of 120 daily values) of 10.1 μg m^{-3} (Hüglin 2000). Contributions of specific primary pollution sources to PM10 could not be detected by chemical analyses. This site is expected to represent a background situation for unpolluted rural areas in Switzerland. Three sites (GUB, KSN, WDK, GMA) have been chosen in and near the city of Zürich. These sites have been studied in detail by BUWAL (1999) and Hüglin (2000) with chemical methods in order to quantify and characterize the different sources of PM10. Site GMA is located in a semi-rural region on the Adlisberg Hill close to Zürich. The measured mean PM10 concentration was 12.5 μg m^{-3} (mean of 3 days). In contrast to CHM, site GMA is located much nearer to possible pollution sources. Site KSN is located in the city centre of Zürich in an urban park area, and is not directly influenced by dominant urban sources. The mean PM10 concentration (mean of 121 daily values) is 24.1 μg m^{-3} (Hüglin 2000). Site WDK is situated near a highly frequented transit road in Zürich city centre (27 000 vehicles/day, 8 per cent of which are heavy trucks). The annual mean PM10 concentration (mean of 59 daily values) at WDK is 43.0 μg m^{-3} (Hüglin 2000). Site GUB is located at the centre of a 3.5 km long motorway tunnel. PM10 is dominated in this tunnel by motor vehicle emissions (e.g. Weingartner *et al.* 1997; John *et al.* 1999). The measured daily mean PM10 concentration was 91.1 μg m^{-3}.

2.2 Sampling

The PM10 samples were collected on fibre-glass filters (Ederol, MG 227/1/60, diameter 150 mm) using a high-volume air sampler (Digitel DHA-80, with a flow of 720 m^3 air per day) with a grain-size-selective air inflow. Grain sizes between 0.3 and 10 μm are filtered. The sampling height was 3 m at sites CHM and WDK and 2 m at all other sites. The PM10 mass was obtained by the difference in weight of the filters before and after air sampling. The filters were stored in a desiccator for 24 hours before each weighing to reach specific climatic conditions (22 °C, 50 per cent relative humidity). Sample CHM was kindly provided by the EMPA (Swiss Federal Laboratories for Material Testing and Research) and sample WDK by the city of Zürich (Office for Environmental and Health Protection). The samples were collected under dry and rather windless conditions between 2000 September and 2002 October. The sampling time was 24 hours for all samples except GMA, which was collected over 72 hours.

2.3 Magnetic measurements

The anhysteretic remanent magnetization (ARM) of the filters that had been folded into 8 cm^3 cubic plastic boxes was measured in order to determine the magnetic mineral components present. ARM and detailed alternating field (AF) demagnetization curves of ARM are considered most suitable for component analysis. Extremely high precision and reproducibility of the experiments are necessary for the analysis of the demagnetization curves. The experiments were performed using a 2 G direct current (DC) SQUID cryogenic magnetometer and a 2 G in-line degausser installed in a magnetically shielded room. Each sample was demagnetized along three orthogonal axes with a maximum AF peak field of 300 mT. After demagnetization an ARM was imparted along the z-axis, in a 0.1 mT DC bias field with a maximum AF peak field of 300 mT and an AF field decay rate of 4 mT s^{-1}. Having removed the sample and switched off the bias field, the sample holder and the coil shield were AF demagnetized with 300 mT. After 2 min, automatic stepwise AF demagnetization was started. The waiting time guaranteed an exact reproducibility of the experiment by always removing the same amount of possible viscous remanence. The samples were demagnetized in 76 steps of increasing field intensity along the direction of the ARM. The steps were approximately evenly distributed on a logarithmic scale (0–20 mT every 1 mT, 21.5–26 mT every 1.5 mT, 28–72 mT every 2 mT, 74–80 mT every 3 mT, 85–150 mT every 5 mT, 156 mT, 163 mT, 170–190 mT every 10 mT, 200–260 mT every 15 mT, 280 mT and 300 mT). The z-axis reading of the magnetometer was taken as a measure of ARM after each demagnetization step. The entire procedure of ARM acquisition and demagnetization was repeated six times for each sample, and nine times for weak samples, in order to increase experimental precision. Comparison of the six- or nine-measurement series facilitated the removal of occasionally occurring outliers. These outliers, typically one to two per sample, were probably produced by interference of the main power with the degaussing unit or the magnetometer. The arithmetic mean of the 'cleaned' measurements was finally accepted as the characteristic demagnetization curve.

3 COMPONENT ANALYSIS

3.1 Theoretical background

The coercivity distribution $f(H)$ of a sample is defined as the absolute value of the first derivative of a stepwise acquisition/demagnetization curve. It shows the magnetic contribution $f(H)\,\mathrm{d}H$ of all minerals with switching fields between H and $H + \mathrm{d}H$ and is formally equivalent to a probability density function (Egli 2003). If the sample contains N groups of magnetic minerals with specific properties, called components, its magnetization is given by a linear combination of the coercivity distributions $f_i\,(H)$ of each component:

$$f(H) = \sum_{i=1}^{N} m_i f_i(H) \tag{1}$$

where m_i is the magnetic contribution of component i. Eq. (1) represents a linear mixing model, which is valid if magnetostatic

interactions between the magnetic grains of different components can be excluded. Yu *et al.* (2002) showed that grain interactions have no detectable effect on the partial ARM additivity, regardless of provenance (natural or synthetic). For this reason, we expect eq. (1) to be valid for the PM10 samples. If the coercivity distribution of individual components is modelled with appropriate functions, eq. (1) can be solved for the magnetic contributions m_i, which are related to different sources of magnetic minerals. The coercivity distribution of an individual component is a bell-shaped function, which is related to the dispersion of physical parameters (grain size, shape) and/or chemical parameters (degree of oxidation) of the magnetic grains. Coercivity distributions of natural and artificial samples have been modelled successfully with logarithmic Gaussian distribution functions (Robertson & France 1994; Kruiver *et al.* 2001; Heslop *et al.* 2002). These functions are symmetrical on a logarithmic field scale. Recently, it has been shown that very precise measurements of coercivity distributions, such as those of the PM10 samples, are better modelled with generalized distribution functions which are characterized by a variable symmetry (Egli 2003, 2004b; Heslop *et al.* 2004).

Egli (2003) introduced so-called maximum entropy skewed generalized Gaussian functions (SGG) to model individual magnetic components identified in natural samples. Accordingly, the coercivity distribution of a component is given by SGG(log H, μ, σ, q), with the shape dependent upon the three parameters μ, σ and q. The first parameter, μ, is the median, and is a measure of the average coercivity of the magnetic particles, which depends on grain size and on chemical composition. A common measure of the coercivity is the median destructive field (MDF); the demagnetizing field at which the magnetization is reduced to half of its initial value. The relation between μ and MDF is given by MDF $= 10^{\mu}$. The second parameter, σ, is a measure of the 'randomness' of a component, and corresponds to the standard deviation if $q = 1$. Typical magnetite components in natural rocks and sediments are characterized by $0.3 < \sigma < 0.5$ (Egli 2004a). Magnetosomes, which are very homogeneous in grain size and composition, are modelled with $\sigma < 0.2$ (Egli 2004a). Coercivity distributions of ARM show values of σ that are typically 10–20 per cent smaller than those calculated from the isothermal remanent magnetization (IRM). Magnetic components with smaller values of σ have less overlapping coercivities and are easier to identify using component analysis. Therefore, ARM is more suitable for component analysis than IRM. The third parameter of a SGG function, q, controls the symmetry of the function and ranges from 0.6 to 1 for natural and anthropogenic magnetite components. These values of q define slightly negatively skewed coercivity distributions (Egli 2004b).

Two SGG functions were used to model the measured coercivity distributions of the PM samples, using the CODICA and GECA software programs developed by Egli (2003). The misfit of models based on only one SGG function is larger than the measurement errors. Such models are not adequate for the characterization of all PM10 samples. The opposite is true for models based on more than two SGG functions: in this case the misfit is much smaller than the measurement errors. These models are not significant and were consequently omitted from the analysis.

3.2 Results

All PM10 samples could be adequately modelled with two magnetic components, hereafter called C1 and C2, and the results (including sample mass, air volume and χ_{ARM}) of this component analysis are shown in Fig. 1 and listed in Table 1. The contribution of the components is expressed as susceptibility of ARM, χ_{ARM}. This parameter is defined as the ARM magnetization, normalized by the net weight of PM, divided by the bias field H_{DC} used to give the ARM; the SI unit is $\mathrm{m^3\ kg^{-1}}$. The concentration of PM10 in the air is usually expressed in $\mu\mathrm{g\ m^{-3}}$, and is obtained by dividing the net mass w_{tot} of the PM collected on the filter with the total air volume V_{air} pumped through the filter. By analogy, we define a dimensionless 'magnetic PM concentration' $m_{\mathrm{C}} = (\chi_{\mathrm{ARM}} w_{\mathrm{tot}})/V_{\mathrm{air}}$.

The coercivity distributions of C1 and C2 of all samples, normalized to $m_{\mathrm{C}} = 1$, are plotted in Fig. 2. The coercivity distributions of each component in different samples have a similar shape in all

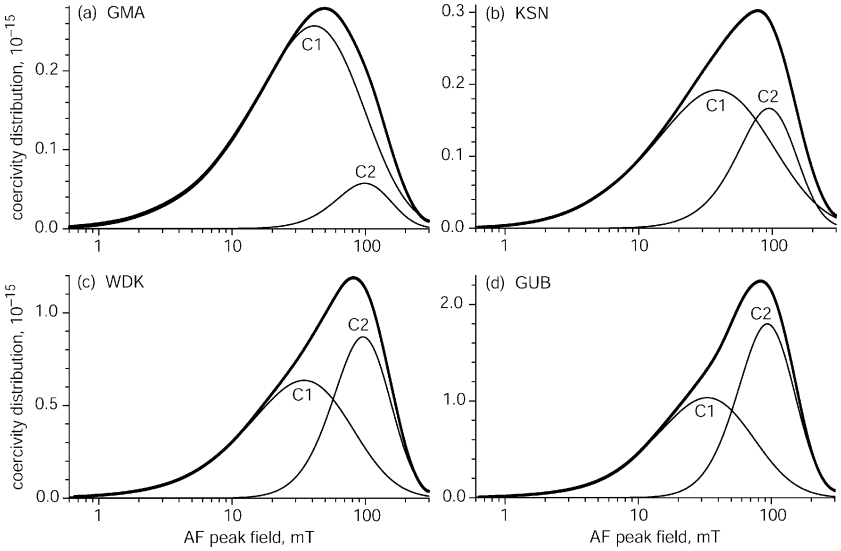

Figure 1. Results of the component analysis performed on the coercivity distribution of the PM10 samples taken in and near Zürich at the following sites: (a) GMA, a woody recreation area outside the city centre; (b) KSN, a park like area in the city centre; (c) WDK, a highly frequented transit road; (d) GUB, a motorway tunnel. Two SGG functions, C1 and C2, have been used to model the coercivity distribution of each sample (thick line). Sampling sites with increasing exposure to pollution sources have been ordered from (a) to (d).

Table 1. Results of the complete component analysis performed with two SGG functions on detailed measurements of the coercivity distribution. (SD = standard deviation).

Sample	Mass,	Vol.,	χ_{ARM}	m_C	Component 1, C1				Component 2, C2			
	w_{tot} (mg)	V_{Air} (m^3)	(μm^3 kg^{-1})	(10^{-15})	χ_{ARM_1} (μm^3 kg^{-1})	μ_1 (log[mT])	σ_1	q_1	χ_{ARM_2} (μm^3 kg^{-1})	μ_2 (log[mT])	σ_2	q_2
CHM	3.5	720	5.00	24.3	4.447	1.525	0.511	0.591	0.584	1.808	0.208	0.998
GMA	81.0	2160	6.50	243.8	5.890	1.520	0.511	0.581	0.660	1.965	0.235	0.659
KSN	30.3	720	5.96	250.8	4.175	1.514	0.507	0.647	1.828	1.934	0.261	0.625
WDK	35.4	720	18.27	898.3	10.546	1.461	0.470	0.607	7.789	1.958	0.235	0.694
GUB	65.6	720	17.21	1568	8.619	1.461	0.420	0.647	8.586	1.948	0.230	0.712
Mean						**1.489**	**0.477**	**0.621**		**1.951**	**0.240**	**0.672**
SD						**0.032**	**0.042**	**0.032**		**0.012**	**0.014**	**0.039**

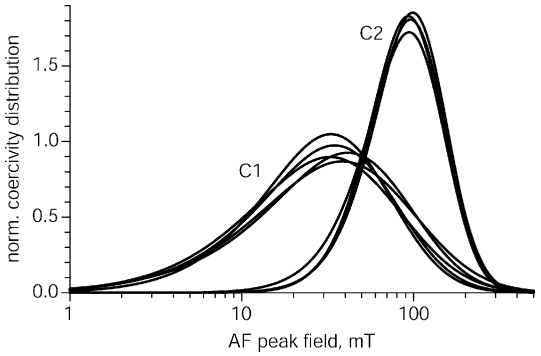

Figure 2. Coercivity distributions of components C1 and C2 found in all samples of Fig. 1. The curves have been normalized so that each component has a unit magnetization. The shape of the coercivity distributions of C1 and C2 is similar in all samples: differences in the bulk properties of the samples arise from variations in the contributions of C1 and C2 to the total magnetization.

samples. This observation supports the validity of the component analysis performed, and suggests that: (1) all samples are affected by common PM sources and (2) the distance from the sources does not significantly affect the magnetic properties of the corresponding magnetic component. The latter point is of particular interest, because the selective transport of finer particles over longer distances may influence grain-size-sensitive magnetic properties. Flanders (1999) observed a change of the bulk coercivity of dust samples collected at increasing distances from fossil fuel power stations. Changes in the bulk magnetic properties of PM can reflect a compositional trend, where the concentration of the high-coercivity fly ash decreases with respect to that of the low-coercivity natural dust. Indeed, the relative contribution of component C2 to the total magnetization of the PM is related to the degree of pollution at the site. In the relatively unpolluted site GMA, outside Zürich, the magnetic contribution of C2 is 15 per cent. At KSN, C2 is responsible for 33 per cent of the magnetic signal, and in the motorway tunnel GUB it reaches 47 per cent. This trend explains the observed change of the bulk MDF of the ARM demagnetization curves from 1.68 ($\hat{=}$ $\approx$ 48 mT) at GMA to 1.92 ($\hat{=}$ $\approx$ 57 mT) at GUB (Fig. 1). For comparison, the MDF of the individual components C1 and C2 is 1.49 ($\hat{=}$ $\approx$ 31 mT) and 1.95 ($\hat{=}$ $\approx$ 89 mT), respectively (Table 1).

3.3 A linear model for the component analysis of PM samples

The characterization of coercivity distributions described above requires precise and time-consuming measurements and is unsuitable for systematic investigation of a large number of PM samples. Because of the constant shape of C1 and C2, the component analysis can be substantially simplified by demagnetizing samples with only a few steps (Egli 2004c). Since the shape of the coercivity distributions of C1 and C2 is fixed in all PM samples, eq. (1) is linear with respect to the m_i, and has constant coefficients. Consider the AF demagnetization curve of Fig. 3a, with four points that correspond to increasing demagnetizing fields given by H_1^-, H_1^+, H_2^- and H_2^+. The last point, H_2^+, may be limited by the maximum field of the AF coil. Let $M(H_1^-)$, $M(H_1^+)$, $M(H_2^-)$, and $M(H_2^+)$ be the measurements after each demagnetization step, and $\Delta M_i = M(H_i^-) - M(H_i^+)$. The magnetic contribution of all minerals in the coercivity intervals $[H_1^-, H_1^+]$ and $[H_2^-, H_2^+]$ is given by ΔM_1 and ΔM_2, respectively (Fig. 3b). The integration of eq. (1) over the two coercivity intervals gives:

$$\begin{pmatrix} \Delta M_1 \\ \Delta M_2 \end{pmatrix} = \begin{pmatrix} a_{11} & a_{12} \\ a_{21} & a_{22} \end{pmatrix} \begin{pmatrix} m_1 \\ m_2 \end{pmatrix} \tag{2}$$

where m_1 and m_2 are the contributions of C1 and C2 to the measured signal and

$$a_{ij} = \int_{H_i^-}^{H_i^+} f_j(H)\,\mathrm{d}H \tag{3}$$

is the contribution of the normalized *i*th component to the *j*th coercivity interval (Fig. 3b). The mean distribution parameters reported in Table 1 can be used to calculate the a_{ij}. In the experiments $H_1^- = 0$ and $H_2^+ = 200$ mT were chosen. Higher fields could have been used for H_2^+; however, truncation effects may affect the coercivity distribution near the maximum alternating field of 300 mT used to impart the ARM (Kruiver *et al.* 2001).

From the theoretical point of view, the choice of H_1^+ and H_2^- is free, and setting $H_1^+ = H_2^-$ would save one demagnetizing step. However, the solution of eq. (2) is influenced by the measurement errors δM_i of ΔM_i, and by model errors δa_{ij} of a_{ij}. Model errors arise from the (small) variability of the components plotted in Fig. 2. The effect of these errors on the solution of eq. (2) depends on the choice of H_1^+ and H_2^-. In order to find the optimal values of H_1^+ and H_2^-, the error propagation has been calculated for different values of H_1^+, H_2^-, and for different compositions of the sample. An average value of 0.2 per cent has been assumed for δM_i from empirical determinations of the measurement errors (Fig. 3c). The δa_{ij} have been calculated from the variance of the mean parameters of each component, reported in Table 1. Results of this error calculation are plotted in Fig. 4. The optimal values of H_1^+ and H_2^- depend only slightly upon the composition of the sample, and $H_1^+ = 20$ mT, $H_2^- = 100$ mT have been chosen. Accordingly, the solution of

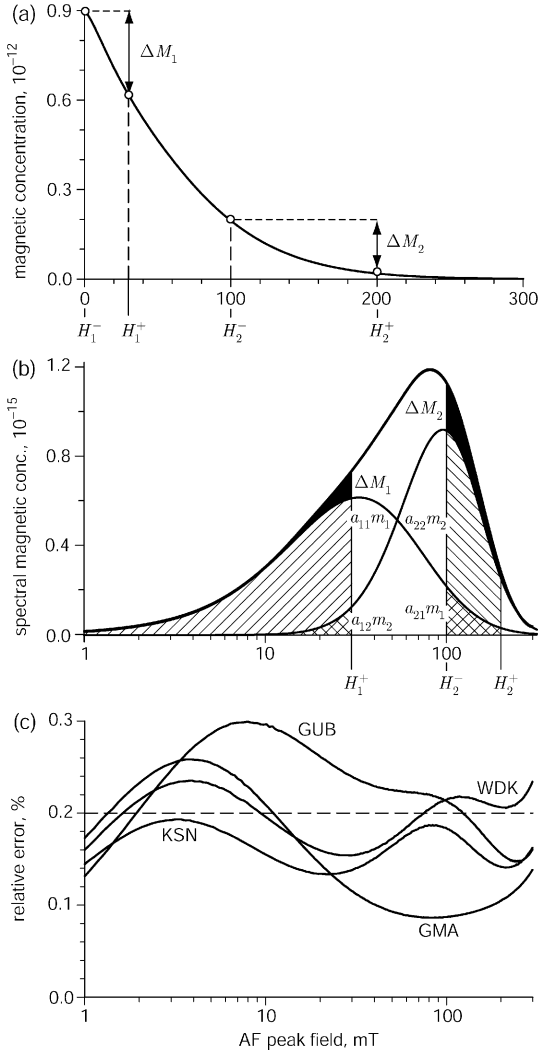

Figure 3. (a) Measurement of four demagnetization steps, defined by the AF peak fields H_1^-, H_1^+, H_2^- and H_2^+. (b) Contributions of components C1 and C2 in the coercivity intervals defined by $[H_1^-, H_1^+]$ and $[H_2^-, H_2^+]$ (dashed areas) to the magnetization of the sample in the same coercivity intervals (black areas). (c) Relative error of the coercivity distributions of GMA, KSN, WDK and GUB, calculated with the software CODICA (Egli 2003). The dashed line indicates the mean error assumed in the text.

eq. (2) is given by:

$$m_1 = +2.983\Delta M_1 - 0.075\Delta M_2$$
$$m_2 = -0.643\Delta M_1 + 2.729\Delta M_2. \quad (4)$$

Results of the simplified component analysis using eq. (4) are reported in Table 2. The magnetic concentrations obtained for C1 and C2 are very similar to those of the complete component analysis described in Section 3.1 (Table 1). In the following, the data reported in Table 2 are used for further interpretation because they represent a realistic result for long-term monitoring of large sample sets.

4 COMPARISON WITH CHEMICAL MEASUREMENTS

PM10 samples from sites CHM, KSN and WDK and from other sites in Switzerland were investigated in detail with chemical methods by Hüglin (2000). The concentration of several elements and chemical compounds was analysed in order to quantify natural and anthropogenic sources of PM10 using a so-called receptor model. According to this model, specific groups of compounds and the dependence of their concentration with time are used as indicators for the emission of certain sources. For example, elemental carbon (EC) and polycyclic aromatic hydrocarbons (PAH), in addition to elements contained in fuel additives such as Pb and Br, are constituents of tail exhaust emissions. Fe, Ba, Cu and Sb particulates are released by vehicle brakes. The receptor model established empirical relationships between PM10 concentrations at investigated sites and identified selected groups of elements for PM source apportionment.

In our study, only one sample from each site has been analysed with magnetic methods, and further investigation is needed on a representative set of samples from each site. Nevertheless, the preliminary results obtained for sites CHM, KSN and WDK offer the possibility to compare estimation of pollution sources by magnetic methods with existing studies. Chemical analysis is sensitive to the mass contribution of the PM10 sources, whereas magnetic investigations are sensitive to the emission of magnetic minerals by each source. Therefore, the sensitivity of chemical and magnetic measurements can be quite different: particles released by vehicle brakes may contribute a few per cent to the total PM10 mass but they are expected to have a large magnetic signal due to their high content of metallic Fe.

4.1 Relative and absolute quantification of urban pollution

Fig. 5(a) shows the linear relationship between the total PM10 and the PM10 from exhaust emissions, according to the receptor model of Hüglin (2000). The same relation has been found between the total PM10 and the magnetic concentration of C2 (Fig. 5a). The contributions of exhaust emissions and of component C2 to PM10 disappear when the total PM10 is as low as 10 $\mu g\ m^{-3}$. This PM10 value corresponds to the annual mean of site CHM, and can be interpreted as the background contribution of natural (global and regional) PM10 sources. A good proportionality has been found between exhaust PM10 and the magnetic concentration of C2 (Fig. 5b). Therefore component C2 is identified with a specific magnetic contribution of exhaust PM10 sources. Based on this assumption, a quantitative

Table 2. Results of the simplified component analysis performed on four-step AF demagnetization curves.

Sample	Measured partial χ_{ARM}		Calculated m_1 and m_2 using eq. (4)		m_1 and m_2 expressed as magnetic concentrations	
	ΔM_1 ($\mu m^3\ kg^{-1}$)	ΔM_2 ($\mu m^3\ kg^{-1}$)	m_{C1}($\mu m^3\ kg^{-1}$)	m_{C2}($\mu m^3\ kg^{-1}$)	$m_{C1}(10^{-15})$	$m_{C2}(10^{-15})$
CHM	1.402	0.531	4.14 ± 0.4	0.55 ± 0.5	20.1 ± 2	2.7 ± 2
GMA	1.877	0.810	5.54 ± 0.5	1.00 ± 0.7	207.7 ± 20	37.6 ± 20
KSN	1.399	1.056	4.09 ± 0.5	1.98 ± 0.6	172.3 ± 20	83.4 ± 20
WDK	3.856	3.608	11.23 ± 1.3	7.37 ± 1.6	552.2 ± 60	362.2 ± 70
GUB	3.079	3.602	8.91 ± 1.2	7.85 ± 1.4	812.1 ± 100	715.3 ± 90

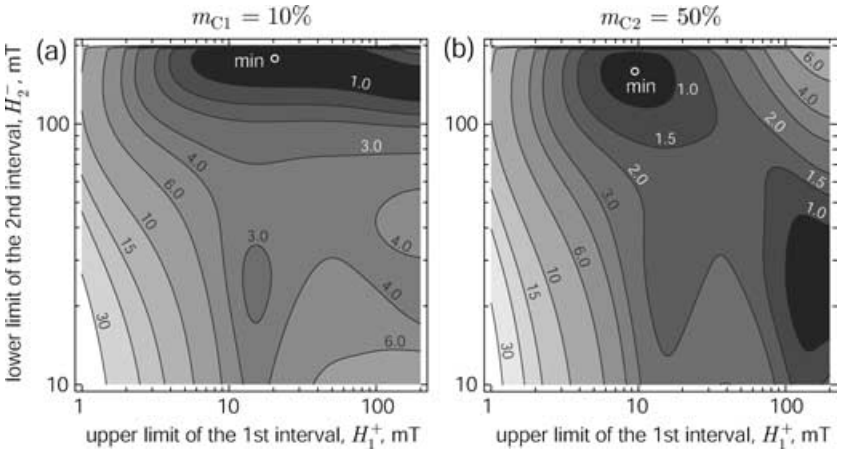

Figure 4. Relative error (per cent) affecting the magnetic concentration m_{C2} of C2 calculated with a simplified component analysis on four-points demagnetization curves for (a) $m_{C2} = 10$ per cent and (b) $m_{C2} = 50$ per cent. The relative error is plotted as a function of the upper limit H_1^+ of the first coercivity interval and the lower limit H_2^- of the second coercivity interval, whereby $H_1^- = 0$ and $H_2^+ = 200$ mT (see Fig. 3). The minimum relative error is marked with a circle.

estimate of the mass contribution of exhaust emissions, c_E, can be deduced empirically from the magnetic concentration of C2, using the proportionality found in Fig. 5(b):

$$c_E(\mu g\ m^{-3}) = (5 \pm 0.7) \times 10^{13} m_{C2}. \quad (5)$$

PM concentrations cannot be determined directly with passive sampling methods which measure the total magnetization of dust accumulated on exposed surfaces such as tree leaves (Flanders 1994; Hannam & Heller 2001). A useful alternative is offered by the measurement of the relative contribution of a specific magnetic component which is related to one or more pollution sources, such as C2. In Fig. 6, relative contribution of exhaust emissions to PM10 at our sites is plotted against the absolute exhaust emissions determined using chemical and magnetic measurements. Good agreement is found between our method and the results of Hüglin (2000). These results support the following simple method for the determination of traffic PM10 concentrations with magnetic measurements on passively sampled sites:

(1) Impart an ARM with >200 mT AF peak field.
(2) Measure the magnetization after 0, 20, 100 and 200 mT AF demagnetization steps.
(3) Normalize the measurements to an initial magnetization of 100.
(4) Use eq. (4) to calculate m_2 in per cent of the total magnetization.
(5) Use the plot of Fig. 6 to obtain the absolute exhaust pipe PM10 value.

The measurement of one sample requires approximately 12 min using a 2 G cryogenic magnetometer with an in-line AF degausser.

The method discussed above for the determination of traffic PM10 is adequate only for sites with a pollution scenario similar to that presented in this paper. Different pollution scenarios may include other pollution sources with different magnetic properties, which have to be completely reanalysed and recalibrated.

4.2 Source attribution of the magnetic components in PM10

In the previous section an empirical proportionality relation has been found between the traffic contribution of PM10 and component C2. In this section, the origin of C1 and C2 will be discussed.

Component C1 is predominant at the relatively unpolluted and remote site CHM. Its coercivity distribution is very similar to that of unaltered loess, which consists mainly of wind-blown natural dust (Evans & Heller 1994; Spassov *et al.* 2003; Egli 2004a). Conversely, the magnetic concentration of C1 increases significantly in polluted sites. For example, the magnetic concentration of C1 at WDK is 27 times higher than the background level at CHM. A part of the increased concentration of component C1 is most likely to be produced by the resuspension of roadside dust by turbulence from passing vehicles and other urban activities. Additional mineral dust is produced by the abrasion of roads. These two factors accounted for 30 per cent of the PM10 emissions in Switzerland during 1997 (Heldstab *et al.* 1999). In addition, an anthropogenic contribution to C1 can also not be excluded. The coercivity distribution of this hypothetical contribution may be similar to that of natural dust because a third component could not be identified with component analysis. Therefore, we make a new approach. We call component P1 the contribution of pollution to component C1, and P2 the contribution of pollution to C2. If N designates the magnetic component related to natural dust, the magnetic concentrations of C1, m_{C1}, and of C2, m_{C2} can be modelled as follows:

$$\begin{aligned} m_{C1} &= m_N + N_T\, r m_N + m_{P1} \\ m_{C2} &= m_{P2} \end{aligned} \quad (6)$$

where $N_T r\, m_N$ is the magnetic contribution of resuspended dust, N_T the traffic intensity, expressed in vehicles per hour and r is a proportionality factor. The primary magnetic contribution of natural dust, m_N, depends on local geological and meteorological settings. According to Fig. 5(a), unpolluted sites in Switzerland are characterized by a PM10 concentration of $\approx$10 $\mu g\ m^{-3}$, a value close to the annual mean of site CHM (Hüglin 2000). If we assume that pollution does not contribute to C1 at CHM, then $m_{C1} = m_N \approx 20.1 \times 10^{-15}$ (see m_{C1} at CHM in Table 2).

In order to verify the model of eq. (6), it is necessary to have an independent estimate of $N_T r$, which can be obtained by comparing the concentrations of an element that is not produced by any pollution source at various sites. A good candidate for such an element is aluminium, since anthropogenic sources of aluminium are negligible (Lantzy & Mackenzie 1979). The same approach as for the magnetic counterpart (see eq. 6) is expected for the total

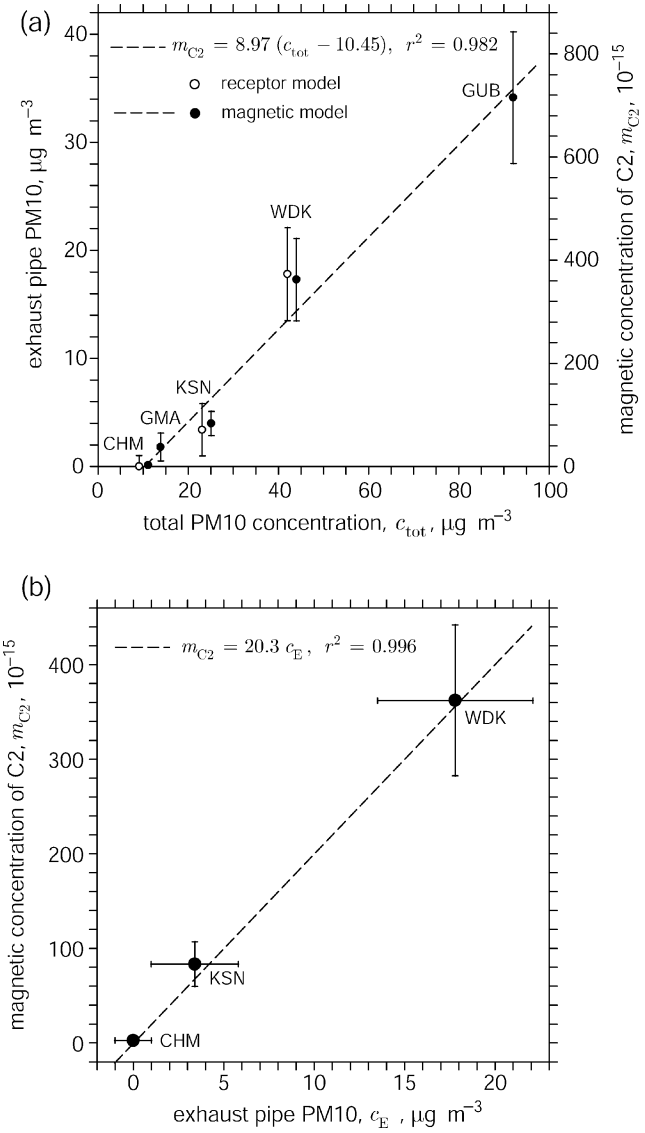

Figure 5. (a) Annual mean PM10 concentration at various sites (abscissa) and the PM10 produced by exhaust emissions (ordinate), both after Hüglin (2000) (circles). For comparison, the magnetic concentration of component C2 (dots) for the samples measured in this paper has been plotted as well. Component C2 and exhaust PM10 show the same linear dependence on the total PM10 concentration, defining a background PM10 concentration of 10.45 μg m^{-3} (abscissa intercept). This concentration is comparable to that of the unpolluted site CHM. (b) Relationship between exhaust pipe emissions c_E according to Hüglin (2000) (abscissa) and the magnetic concentration m_{C2} of component C2 (ordinate). The proportionality between c_E and m_{C2} can be used to determine exhaust pipe emissions from magnetic measurements (see eq. 5).

concentration of aluminium, c_{Al}:

$$c_{Al} = c_{Al_B} + N_T r c_{Al_B}, \tag{7}$$

c_{Al_B} being the background aluminium concentration. The anthropogenic term is assumed to be zero (see above). $N_T r$ can be calculated from eq. (7). c_{Al_B} is known from the linear relationship between c_{Al} and the concentration of road dust, c_{RD}, normalized by the concentration of natural dust, c_{ND} (Fig. 7a), both obtained with the chemical receptor model. Estimates of road and natural dust concentrations in PM10 are reported in Hüglin (2000) for five

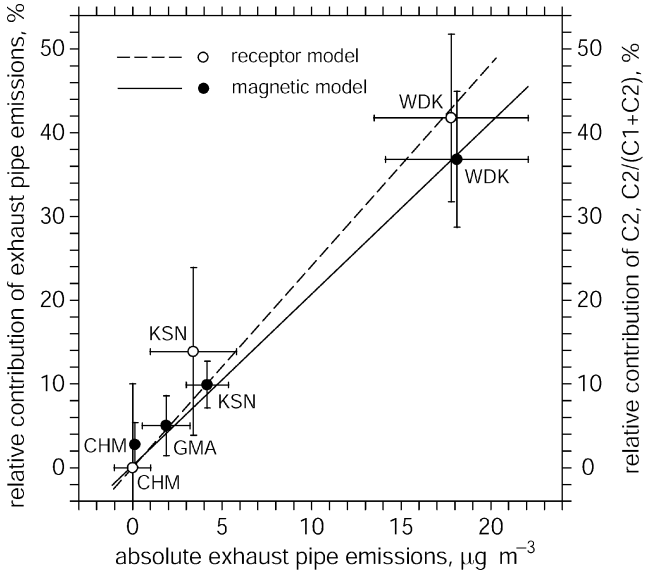

Figure 6. Absolute (abscissa) and relative (ordinate) contribution of exhaust emissions in PM10. Open circles and the dashed best-fit line refer to the analysis of Hüglin (2000). Solid dots and the solid best-fit line refer to the results of magnetic measurements, whereby exhaust emissions were identified with component C2.

sites in Switzerland. A linear fit of c_{Al} versus c_{RD}/c_{ND} gives a background Al concentration of $c_{Al_B} = 13.2$ ng m^{-3} (Fig. 7a), close to the measured mean annual Al concentration of 14 ng m^{-3} at CHM (Hüglin 2000). Solving eq. (7) for $N_T r$ and inserting into eq. (6), yields for m_{C1}:

$$\begin{aligned} m_{C1} &= m_N + (b/c_{Al_B}) c_{RD}/c_{ND} m_N + m_{P1} \\ m_{C1} &= (20.1 + 47.5 c_{RD}/c_{ND}) \times 10^{-15} + m_{P1}. \end{aligned} \tag{8}$$

The constant b is the correlation coefficient obtained from the fit in Fig. 7(a) and amounts to 31.2.

If P1 and P2 are products of the same source, a proportionality relation is expected between m_{P1} and m_{P2} (Fig. 7b). A least-squares linear fit gives $m_{P1} = (1.15 \pm 0.03)\, m_{P2}$. The magnetic concentration of all components is then given by:

$$\begin{aligned} m_N &= m_{C1} - 1.15 m_{C2} \\ m_{P1} &= 1.15 m_{C2} \\ m_{P2} &= m_{C2}. \end{aligned} \tag{9}$$

The magnetic concentrations of N, P1 and P2 can now be estimated for all sites where c_{RD} and c_{ND} are known (Table 3). An individual source attribution of P1 and P2 is not possible with the present data because the ratio of these two components is the same in all sites. Possible magnetization carriers for P1 and P2 are (1) fly ash particles produced by combustion processes, (2) metallic and/or oxidized iron released by brakes and other abraded parts of vehicles and (3) debris from tyre wear. Fly ash particles are characterized by a relatively high coercivity, because of the high stress developed during rapid cooling after formation (Flanders 1999). The release of iron and oxidized iron by rail brakes has been investigated by BUWAL (2002). Particles released by brakes are relatively coarse-grained; nevertheless, about 50 per cent of the emissions consist of PM10. The coercivity of these particles has not been investigated. Coarse iron particles should fall into the multidomain range, and a low coercivity might be expected if the coercivity is not increased by surface oxidation. This latter process also affects natural magnetite grains

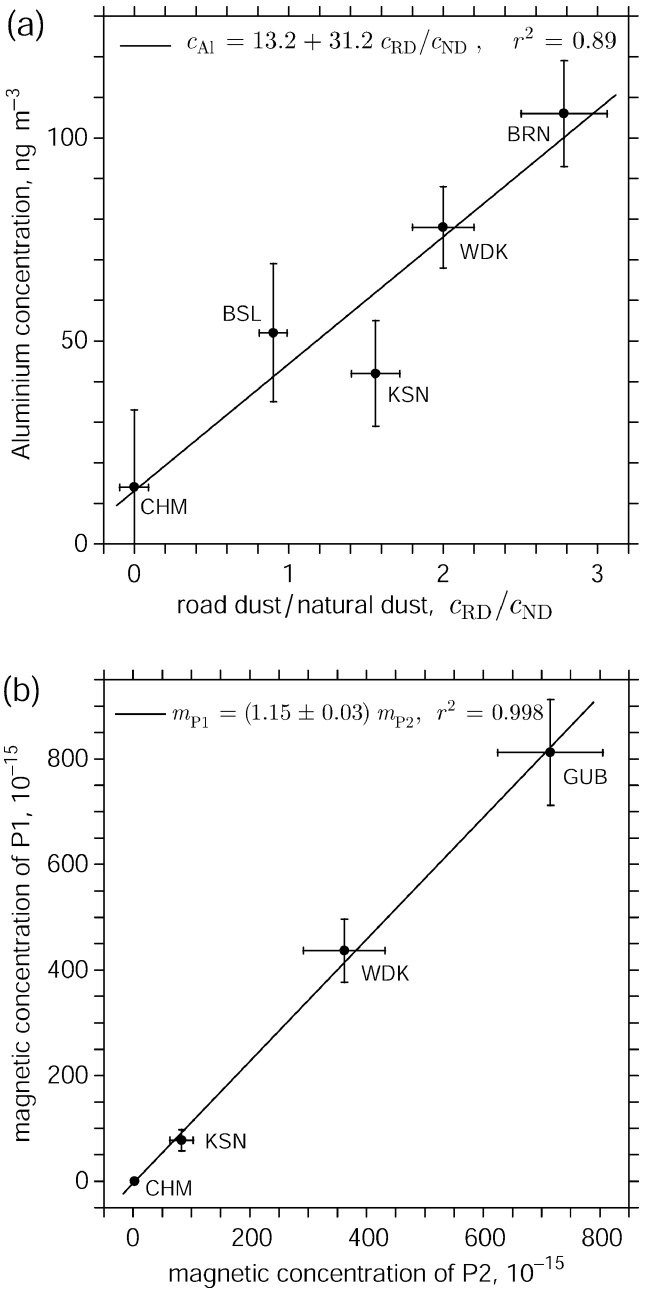

Figure 7. (a) Relationship between the concentration of natural dust in PM10, which is assumed to be proportional to the aluminium concentration (ordinate), and the traffic intensity (abscissa), estimated by the ratio between road dust and natural dust, both after Hüglin (2000). BSL and BRN refer to sampling sites in the cities of Basel and Berne, respectively. The linear relation shown by the plot is compatible with a model for dust resuspension, which assumes the amount of resuspended natural dust to be proportional to the traffic intensity. The ordinate intercept at $c_{Al} = 13.2$ ng m^{-3} defines a background Al concentration, c_{Al_B}, that is similar to the Al concentration in PM10 from the unpolluted site CHM. (b) The coercivity distribution of the pollution component P1 is similar to that of natural dust, and P1 cannot be quantified with component analysis. An indirect estimate of P1 is obtained by subtracting the contribution of natural dust from C1. According to this estimation, P1 and P2 are proportional, as shown in the plot; a common source of P1 and P2 is suggested.

(van Velzen & Dekkers 1999), and a portion of the brake emissions could have a coercivity distribution that is similar to natural dust. The magnetic properties of debris from tyre wear are controlled by traces of iron oxides and iron sulphides that may be contained in the tyres. Studies about the magnetic properties of products of tyre wear have not been found in the literature.

4.3 Comparison of the magnetic results with chemical analysis

The relationship between the total magnetic concentration of pollutants, $m_P = m_{P1} + m_{P2}$, and the occurrence of specific elements indicative of road traffic emissions is shown in Table 4. Excellent linear relationships have been found for Fe, Ba, Cu, Mo, Sb, Br and elemental carbon, EC. Iron is contained in the majority of all minerals that are able to carry a remanent magnetization, and a good correlation between mass concentration and magnetization is expected for this element. Fe, Ba, Cu, Mo and Sb are released by vehicle brakes, and with the exception of Fe are specific for this pollution source. The mass concentrations of brake-specific elements are proportional to m_P. Elemental carbon is contained in exhaust emissions of diesel engine vehicles and in road emissions (road dust, road abrasion), and is also emitted by heating installations in buildings and during wood firing. Consequently, road traffic is not the only source of EC, and a background concentration of 310 ng m^{-3} can be deduced from Table 4. A proportionality relation is also found between m_P and Br, an additive of unleaded fuel. Linear correlations between $m_P (= m_{P1} + m_{P2})$ and various elements measured by Hüglin (2000) are listed in Table 4. Significant correlations are obtained only for the elements discussed above.

5 CONCLUSIONS

The magnetization of PM10 samples was analysed in order to find a relation with the concentration of specific pollution sources in Switzerland. Detailed AF demagnetization curves of ARM of remote to kerbside sites were modelled with two magnetic components, C1 and C2. After characterization of the coercivity distributions of C1 and C2, a simple method for the quantification of C1 and C2 was developed. This method is based on four-step demagnetization curves, which can be measured in 12 min using a 2 G cryogenic magnetometer and an in-line AF degausser. A large number of samples can be analysed in this way if basic assumptions are maintained.

The magnetic contribution of C2 (=P2) was proportional to the chemically estimated PM10 mass contribution of exhaust emissions. An estimation of the amount of resuspended dust was used to evaluate the origin of component C1, which dominates in weakly polluted sites. However, the comparison between the samples shows that C1 is also related to pollution sources. We suggest that C1 is most probably the sum of two distinct components, N and P1, with similar magnetic properties that cannot be resolved with component analysis. Component N is composed of natural dust, which is partly resuspended by traffic and other human activities in urban areas. The magnetic contribution of P1 is proportional to P2, suggesting that these two components are related to the same traffic related pollution source P (= P1 + P2).

Elements emitted by traffic-related PM10 sources, such as Fe, Ba, Cu, Mo, EC and Br, correlate very well with P ($r^2 > 0.998$). From these considerations it was possible to establish empirical relations between the magnetic contribution of P on the one hand and the mass contribution of traffic emissions on the other. Thus

Table 3. Source attribution for the magnetic measurements of PM10 samples. Component N is related to natural dust; components P1 and P2 are related to traffic pollution. The ARM susceptibilities of N and P1 + P2 have been calculated as best-fit proportionality relation between their magnetic contributions and their mass contribution in CHM, KSN and WDK. The mass contribution of N has been identified as road dust (excluding exhaust emissions from road traffic) and road salt (including resuspended road dust); the mass contribution of P1 + P2 with exhaust emissions is according to the emission categories given in Hüglin (2000).

Sample	Magnetic concentration, m_C (10^{-15})				P1 + P2
	Total	N	P1	P2	(per cent)
CHM	22 ± 0.1	20 ± 2	0 ± 2	2 ± 2	10 ± 10
GMA	244 ± 0.5	164 ± 20	43 ± 10	38 ± 10	33 ± 4
KSN	251 ± 0.5	95 ± 9	78 ± 20	83 ± 20	64 ± 8
WDK	898 ± 2	115 ± 10	437 ± 60	362 ± 60	89 ± 7
GUB	1568 ± 3	0	812 ± 100	715 ± 100	100
χ_{ARM}(10^{-6} m^3 kg^{-1})		16 ± 3			44.5 ± 0.8

Table 4. Correlation between the magnetic concentration of pollution, m_P, and various substances analysed by Hüglin (2000). The correlation is based on samples CHM, KSN and WDK. Entries in bold type indicate a significant correlation at a 95 per cent confidence level.

Substance	[Element, (ng m^{-3})] $= a + 10^{-15} \times b m_P$		Correlation	Occurrence
	a	b	coefficient, r^2	
Nitrate	$(5.6 \pm 3) \times 10^2$	$(2.7 \pm 0.6) \times 10^0$	0.950	Secondary aerosols
Sulphate	$(1.9 \pm 0.5) \times 10^3$	$(1.8 \pm 1) \times 10^0$	0.778	
Na^+	$(1.04 \pm 0.05) \times 10^2$	$(1.5 \pm 0.1) \times 10^{-1}$	0.994	Road and marine salt
Mg^{2+}	$(2.42 \pm 0.04) \times 10^1$	$(3.3 \pm 0.08) \times 10^{-2}$	0.9994	
Cl^-	$(0 \pm 3) \times 10^0$	$(9.0 \pm 0.7) \times 10^{-2}$	0.990	
Al	$(2.1 \pm 0.9) \times 10^1$	$(7.4 \pm 0.2) \times 10^{-2}$	0.933	Mineral dust
Ca	$(9.0 \pm 4) \times 10^1$	$(3.1 \pm 0.9) \times 10^{-1}$	0.931	
EC	$\mathbf{(3.1 \pm 0.8) \times 10^2}$	$\mathbf{(8.2 \pm 0.2) \times 10^0}$	**0.9996**	**Combustion product**
OC	$(1.3 \pm 0.6) \times 10^3$	$(5.7 \pm 1) \times 10^0$	0.946	
Br	$\mathbf{(4.2 \pm 0.5) \times 10^1}$	$\mathbf{(4.5 \pm 0.2) \times 10^{-1}}$	**0.9984**	**Fuel additive**
Fe	$\mathbf{(4.2 \pm 2) \times 10^1}$	$\mathbf{(1.89 \pm 0.05) \times 10^0}$	**0.9993**	Mineral dust, **Vehicle brakes**
Ba	$\mathbf{(0 \pm 5) \times 10^{-1}}$	$\mathbf{(3.6 \pm 0.1) \times 10^{-2}}$	**0.9985**	**Vehicle brakes**
Cu	$\mathbf{(0 \pm 1) \times 10^0}$	$\mathbf{(9.5 \pm 0.2) \times 10^{-2}}$	**0.9984**	
Mo	$\mathbf{(0 \pm 6) \times 10^{-2}}$	$\mathbf{(6.4 \pm 0.1) \times 10^{-3}}$	**0.9995**	
Sb	$(0 \pm 5) \times 10^{-1}$	$(1.1 \pm 0.1) \times 10^{-2}$	0.9906	
Ni	$(4.7 \pm 2) \times 10^{-1}$	$(3.1 \pm 0.5) \times 10^{-3}$	0.975	Products of
Mn	$(1.9 \pm 1) \times 10^0$	$(1.8 \pm 0.3) \times 10^{-2}$	0.979	combustion and
V	$(5.7 \pm 1) \times 10^{-1}$	$(8.1 \pm 2) \times 10^{-4}$	0.938	industrial processes
Pb	$(7.2 \pm 3) \times 10^0$	$(4.9 \pm 0.6) \times 10^{-2}$	0.984	
K	$(9.0 \pm 3) \times 10^1$	$(1.1 \pm 0.8) \times 10^{-1}$	0.680	Various sources
Zn	$(9 \pm 6) \times 10^0$	$(3.5 \pm 1) \times 10^{-2}$	0.892	
As	$(1.9 \pm 1) \times 10^{-1}$	$(5.4 \pm 2) \times 10^{-4}$	0.811	

magnetic measurements can be calibrated for quantitative estimation of the PM10 mass concentration from traffic pollution sources. The relative magnetic contribution of P2 can be used as an inexpensive and fast proxy for systematic pollution monitoring of wide areas with passive sampling methods (e.g. tree leaves).

The results of our study are based on measurements from only a few sites. They encourage thorough investigation of more sites related to different pollution scenarios in order calibrate magnetic measurements for pollution monitoring.

ACKNOWLEDGMENTS

We would like to thank Christoph Hüglin (EMPA) for providing samples from Chaumont, Andreas Schlatter (road maintenance Kanton Zürich) for permission to sample in the motorway tunnel (Gubristtunnel), Susanne Schlatter (Office for Environmental and Health Protection Zürich) for using the high-volume air sampler and for providing the WDK sample and Bruno Busato (Health Office Winterthur) for the PM10 mass estimation. We are grateful to Jürgen Matzka and an anonymous reviewer for careful and constructive reviews.

REFERENCES

BUWAL, 1999. *Modellierung der PM10-Belastung in der Schweiz*, Schriftreihe Umwelt, 310, Bundesamt für Umwelt, Wald und Landschaft, Bern.

BUWAL, 2002. *PM10-Emissionen des Verkehrs*, Statusbericht Teil Schienenverkehr, Umwelt-Materialien, 144, Bundesamt für Umwelt, Wald und Landschaft, Bern.

Cornell, R.M. & Schwertmann, U., 1996. *The Iron Oxides* VCH, Weinheim.

Dekkers, M.J. & Pietersen, H.S., 1992. Magnetic properties of low-Ca fly ash: a rapid tool for Fe-assessment and survey for potentially hazardous elements, in, *Advanced Cementitious Systems: Mechanisms and Properties*, Materials Research Society Symposium Proceedings 245, pp. 34–47, eds Glasser, F.P., McCarthy, G.J., Young, J.F., Masson, T.O. & Pratt, P.L., Materials Research Society, Pittsburgh, PA.

Diabaté, S., Mülhopt, S., Paur, H.-R., Wottrich, R. & Krug, H.F., 2002. *In vitro* effects of incinerator fly ash on pulmonary macrophages and epithelial cells, *Int. J. Hyg. Environ. Health,* **204,** 323–326.

Dreher, K.L., Richhard, H.J., Lehmann, J.R., Richards, J.H. & McGee, J.K., 1997. Soluble transition metals mediate residual oil fly ash induced acute lung injury, *J. Toxicol. Environ. Health,* **50,** 285–305.

Egli, R., 2003. Analysis of the field dependence of remanent magnetization curves, *J. geophys. Res.,* **108**, (B2), 2081, doi:10.1029/2002JB002023.

Egli, R., 2004a. Characterisation of individual rock magnetic components by analysis of remanence curves, 1. Unmixing natural sediments, *Stud. Geophys. Geod.*, **48,** 391–446.

Egli, R., 2004b. Characterisation of individual rock magnetic components by analysis of remanence curves, 2. Rock magnetism of individual components, *Phys. Chem. Earth,* **29,** 851–867.

Egli, R., 2004c. Characterisation of individual rock magnetic components by analysis of remanence curves, 3. Biogenic magnetite and natural processes in lakes, *Phys. Chem. Earth,* **29,** 869–884.

Evans, M.E. & Heller, F., 1994. Magnetic enhancement and paleoclimate: study of a loess/paleosol couplet across the Loess Plateau of China, *Geophys. J. Int.,* **117,** 257–264.

Flanders, P.J., 1994. Collection, measurement, and analysis of airborne magnetic particulates from pollution in the environment (invited), *J. appl. Phys.,* **75,** 5931–5936.

Flanders, P.J., 1999. Identifying fly ash at a distance from fossil fuel power stations, *Environ. Sci. Technol.,* **33,** 528–532.

Freer-Smith, P.H., Holloway, S. & Goodman, A., 1997. The uptake of particulates by an urban woodland: site description and particulate composition, *Environ. Pollut.,* **95,** 27–35.

Hannam, J. & Heller, F., 2001. Magnetic investigations of roadside leaves in Zürich, Switzerland, *MAGazine Newsletter,* **4,** 4.

Heldstab, J., de Haan, P., Künzle, T. & Filliger, P., 1999. PM10 map and population exposure for Switzerland, 6th International Conference on Harmonization within Atmospheric Dispersion Modelling for Regulatory Purposes (HARMO), 11–14 October 1999, Rouen, France, *Int. J. Environ. Pollution,* **16,** Special Issue, No. 1–6.

Heslop, D., Dekkers, M.J., Kruiver, P.P. & van Oorschot, I.H.M., 2002. Analysis of isothermal remanent magnetization acquisition curves using the expectation-maximization algorithm, *Geophys. J. Int.,* **148,** 58–64.

Heslop, D., McIntosh, G. & Dekkers, M.J., 2004. Using time and temperature dependant Preisach models to investigate the limitations of modelling isothermal remanent magnetisation acquisition curves with cumulative log Gaussian functions, *Geophys. J. Int.,* **157,** 55–63.

Hüglin, C., 2000. *Anteil des Strassenverkehrs an den PM1- und PM2.5 Immissionen*, Berichte des NFP 41 Verkehr und Umwelt, Bericht C4, BUWAL, Bern, 1–89.

Hunt, A., Jones, J. & Oldfield, F., 1984. Magnetic measurements and heavy metals in atmospheric particulates of anthropogenic origin, *Sci. Total Environ.,* **33,** 129–139.

John, C., Friedrich, R., Staehelin, J., Schläpfer, K. & Stahel, W.A., 1999. Comparison of emission factors for road traffic from a tunnel study (Gubrist tunnel, Switzerland) and from emission modelling, *Atmos. Environ.,* **33,** 3367–3376.

Kapička, A., Jordanova, N., Petrovský, E. & Ustjak, S., 2001. Effect of different soil conditions on magnetic parameters of power-plant fly ashes, *J. appl. Geophys.,* **48,** 93–102.

Kruiver, P.P., Dekkers, M.J. & Heslop, D., 2001. Quantification of magnetic coercivity components by the analysis of acquisition curves of isothermal remanent magnetization, *Earth planet. Sci. Lett.,* **189,** 269–276.

Lantzy, R. & Mackenzie, F.T., 1979. Atmospheric trace metals: global cycles and assessment of man's impact, *Geochim. Cosmochim. Acta*,**43,** 511–525.

Matzka, J., 1997. Magnetische, elektronenmikroskopische und lichtmikroskopische Untersuchungen an Stäuben und Aschen sowie an einzelnen Aschepartikeln, *Diploma Thesis*, Institut für Allgemeine und Angewandte Geophysik, Universität München, München.

Matzka, J. & Maher, B.A., 1999. Magnetic biomonitoring of roadside tree leaves: identification of spatial and temporal variations in vehicle-derived particulates, *Atmos. Environ.,* **33,** 4565–4569.

Moreno, E., Sagnotti, L., Dinares-Turell, J., Winkler, A. & Cascella, A., 2003. Biomonitoring of traffic air pollution in Rome using magnetic properties of tree leaves, *Atmos. Environ.,* **37,** 2967–2977.

Muxworthy, A.R., Matzka, J. & Petersen, N., 2001. Comparison of magnetic parameters of urban atmospheric particulate matter with pollution and meteorological data, *Atmos. Environ.,* **35,** 4379–4386.

Muxworthy, A.R., Schmidbauer, E. & Petersen, N., 2002. Magnetic properties and Mössbauer spectra of urban atmospheric particulate matter: a case study from Munich, Germany, *Geophys. J. Int.,* **150,** 558–570.

Muxworthy, A.R., Matzka, J., Davila, A.F. & Petersen, N., 2003. Magnetic signature of daily sampled urban atmospheric particles, *Atmos. Environ.,* **37,** 4163–4169.

Robertson, D.J. & France, D.E., 1994. Discrimination of remanence-carrying minerals in mixtures, using isothermal remanent magnetisation acquisition curves, *Phys. Earth planet. Inter.,* **82,** 223–234.

Shu, J., Dearing, J.A., Morse, A.P., Yu, L.Z. & Yuan, N., 2001. Determining the sources of atmospheric particles in Shanghai, China, from magnetic and geochemical properties, *Atmos. Environ.,* **35,** 2615–2625.

Smith, K.R., Veranth, J.M., Hu, A.A., Lighty, J.S. & Aust, A.E., 2000. Interleukin-8 levels in human lung epithelial cells are increased in response to coal fly ash and vary with the bioavailability of iron, as a function of particle size and source of coal, *Chem. Res. Toxicol.,* **13,** 118–125.

Spassov, S., Heller, F., Kretzschmar, R., Evans, M.E., Yue, L.P. & Nourgaliev, D.K., 2003. Detrital and pedogenic magnetic mineral phases in the loess/palaeosol sequence at Lingtai (Central Chinese Loess Plateau), *Phys. Earth planet. Inter.,* **140,** 255–275.

van Maanen, J.M.S., Borm, P.J.A., Knaapen, A., van Herwijnen, M., Schildermann, P.A.E.L., Smith, K.R., Aust, A.E. & Tomatis, M., 1999. In vitro effects of coal fly ashes: hydroxyl radical generation, iron release, and DNA damage and toxicity in rat lung epithelial cells, *Inhal. Toxicol.,* **11,** 1123–1141.

van Velzen, A.J. & Dekkers, M.J., 1999. Low-temperature oxidation of magnetite in loess-paleosol sequences: a correction of rock magnetic parameters, *Stud. Geophys. Geod.,* **43,** 357–375.

Weingartner, E., Keller, C., Stahel, W.A., Burtscher, H. & Baltensperger, U., 1997. Aerosol emission in a road tunnel, *Atmos. Environ.,* **31,** 451–462.

Xie, S.J., Dearing, J.A. & Bloemendal, J., 2000. The organic matter content of street dust in Liverpool, UK, and its association with dust magnetic properties, *Atmos. Environ.,* **34,** 269–275.

Yu, Y., Dunlop, D.J. & Özdemir, Ö., 2002. Partial anhysteretic remanent magnetization in magnetite, 1: Additivity, *J. geophys. Res.,* **107,** doi:10.1029/2001JB001249.